

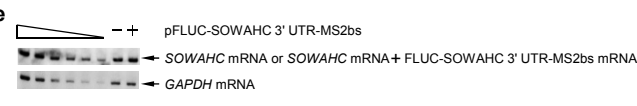
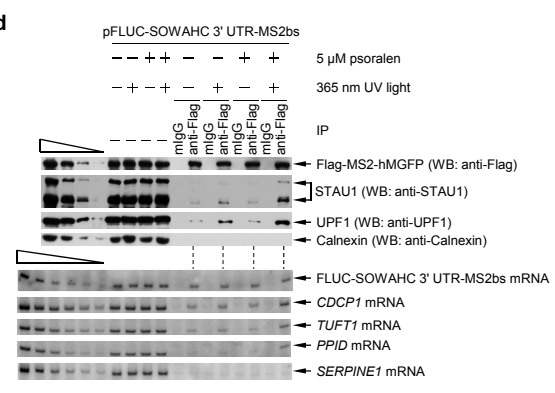
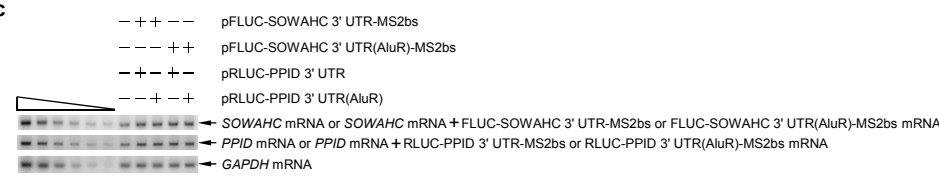
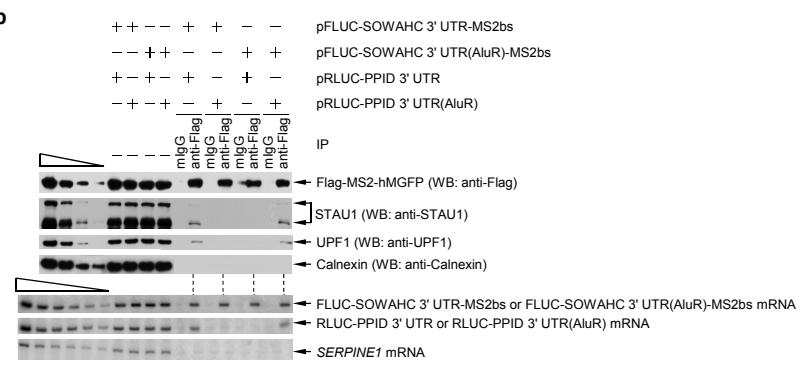
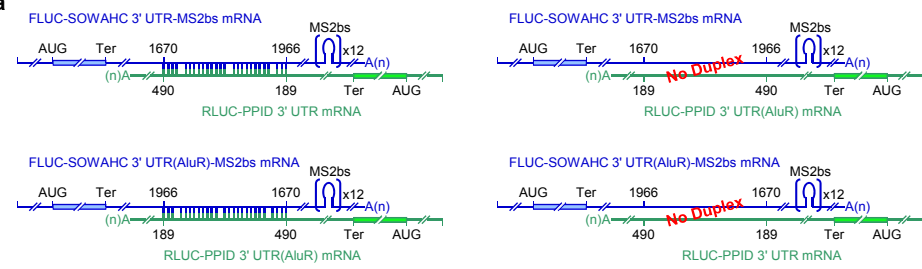
Supplementary Information

mRNA–mRNA duplexes that auto-elicited Staufen1-mediated mRNA decay

Chenguang Gong, Yalan Tang & Lynne E. Maquat

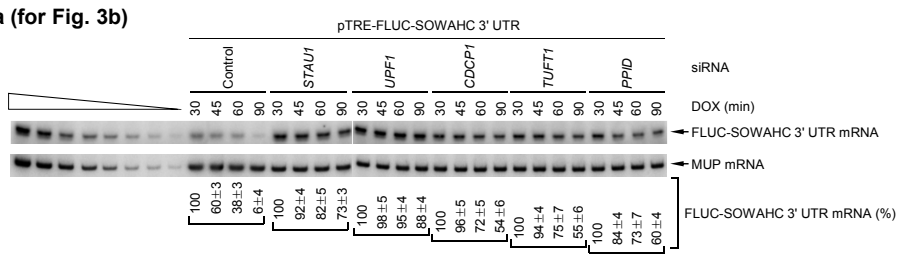
Supplementary Figure 1 | Predicted base-pairing between the Alu elements within the 3' UTRs of the specified mRNAs, and evidence that *SOWAHC* mRNA is translated; Phosphorimages of RT-sqPCR data that were presented as histograms with error bars in the denoted Figure, and RT-qPCR data using RT samples analyzed in denoted Figure; Position of mRNA–mRNA duplex formation with a 3' UTR influences whether the duplex will bind STAU1 and trigger SMD; Repeat of experiments shown in Fig. 1b using different siRNAs. a, Perl program “RNA_RNA_anneal” was used to predict the intermolecular duplexes formed via base-pairing of partially complementary 3' UTR Alu elements in the specified mRNAs. **b**, Table of ΔG values (kcal/mol) for duplexes that putatively form between the 3' UTR Alu elements of the specified mRNAs. **c**, Western blot (WB) of lysates of HeLa cells transiently expressing the denoted siRNA, demonstrating that *SOWAHC* siRNA downregulates *SOWAHC* (i.e., FLJ21870) protein production. **d**, Published (see reference #) or predicted effects on cell motility upon downregulation of the specified mRNA. **e-h**, Phosphorimages of RT-sqPCR data and RT-qPCR data. It is worth noting that, based on the intensity of each RT-sqPCR product and the number of PCR cycles, the abundance of the six mRNAs assayed is roughly comparable. **i**, Diagrams of the duplexes predicted to form between two FLUC reporter mRNAs (FLUC-artificial 3' UTR mRNA and FLUC-artificial 3' UTR (shuffle) mRNA) and the specified antisense (AS) artificial lncRNA. 3' UTR sequences labeled 1-68 in the FLUC-artificial 3' UTR mRNA is shuffled in the FLUC-artificial 3' UTR (shuffle) mRNA so that sequences 39-68 are followed immediately by sequences 1-38. Thus, each reporter mRNA harbors either 68- or 30-nucleotides, respectively residing 74- or 44-nucleotides, downstream of its termination codon (Ter), that are perfectly complementary to the lncRNA with which it is diagrammed to duplex. **j**, Computationally calculated ΔG values for each putative duplex shown in **i**. **k**, Western blot

(WB), using the designated antibody (α), of lysates of HeLa cells that had been transiently transfected with the specified siRNA and, subsequently, the appropriate pFLUC reporter and AS lncRNA effector plasmids to produce the denoted mRNA–lncRNA duplex, and the reference pRLUC plasmid. Calnexin serves as a loading control. **l**, RT-sqPCR analyses of each FLUC reporter mRNA and RLUC mRNA from the same lysates analyzed in **k**. **m**, Histogram representation of data shown in **l**. The level of each reporter FLUC reporter mRNA was normalized to the level of reference RLUC mRNA, and normalized levels in the presence of Control siRNA were defined as 100. **n**, Western blot (upper) or RT-sqPCR (lower) of lysates of formaldehyde-crosslinked HeLa cells that had been transiently transfected as in **k**, except that pSTAU1-HA₃ was also included, before (–) or after IP with anti-HA or as a control for nonspecific IP rat immunoglobulin G (rIgG). **o**, Essentially as Fig. 1b except alternative siRNAs were used to downregulate each target. Error bars, s.e.m.; # of independently performed experiments = 3; P < 0.05 (one-tail *t*-test).



Supplementary Figure 2 | Additional evidence for mRNA–mRNA interactions via Alu-element base-pairing. a, Diagrams of predicted duplexes formed between FLUC-SOWAHC 3' UTR-MS2bs and RLUC-PPID 3' UTR, in which both Alu elements are in the proper orientation, or FLUC-SOWAHC 3' UTR(AluR)-MS2bs mRNA and RLUC-PPID 3' UTR(AluR) mRNA, in which both Alu elements are in the reversed orientation (R). No duplexes are predicted to form between mRNAs that contain Alu elements in non-complementary orientations. **b,** Essentially as Fig. 2b except cells were transfected with the specified plasmids. **c,** Using samples analyzed in b, demonstration that transiently introduced plasmids produced mRNA at ~0.6-fold the level of its cellular counterpart under conditions where ~90% of cells were transfected [GFP fluorescent assays of cultured cells that had been transiently transfected with pEGFP-N1 (Clontech Labs), data not shown]. **d,** Essentially as Fig. 2b except cells were (+ psoralen) or were not (– psoralen) exposed to 5µM psoralen under conditions that did (+ 365 nm UV light) or did not (– 365 nm UV light) promote crosslinking. **e,** Using samples analyzed in d, demonstration that transiently introduced plasmids produced mRNA at ~0.6-fold the level of its cellular counterpart under conditions where ~90% of cells were transfected (data not shown). # of independently performed experiments = 3; P <0.05 (one-tail *t*-test).

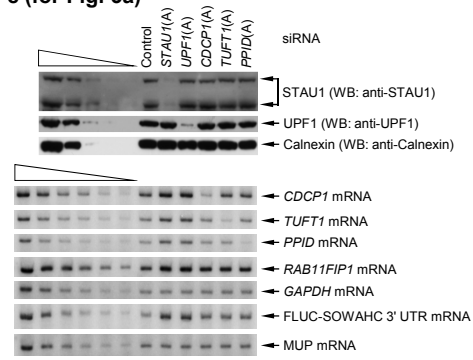
a (for Fig. 3b)



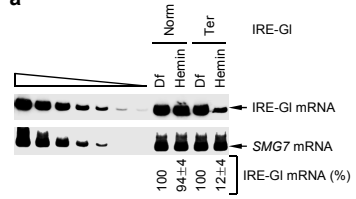
b (for Fig. 3b)

siRNA	DOX (min)	30	45	60	90
Control	100	64±7	34±7	4±2	
STAU1	100	95±6	88±4	78±7	
UPF1	100	99±8	96±6	90±4	
CDCP1	100	92±5	77±9	55±7	
TUFT1	100	91±11	74±5	51±8	
PPID	100	81±9	71±10	61±10	

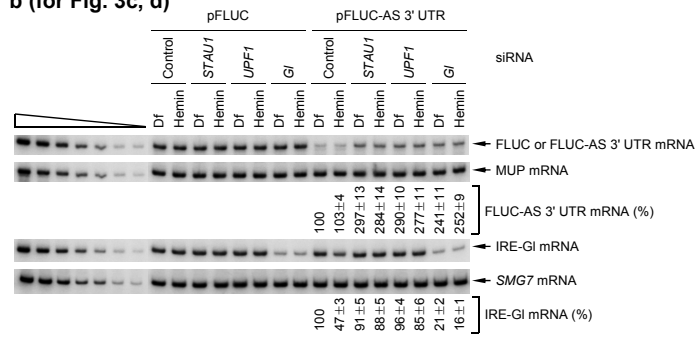
c (for Fig. 3a)



Supplementary Figure 3 | Phosphorimages of RT-sqPCR data that were presented as histograms with error bars in the denoted Figure, and RT-qPCR data using RT samples analyzed in denoted Figure; Repeat of experiments shown in Fig. 1b using different siRNAs. a, Phosphorimages of RT-sqPCR data. b, RT-qPCR data. c, Essentially as Fig. 3a except alternative siRNAs were used. # of independently performed experiments = 3, P <0.05 (one-tail *t*-test).



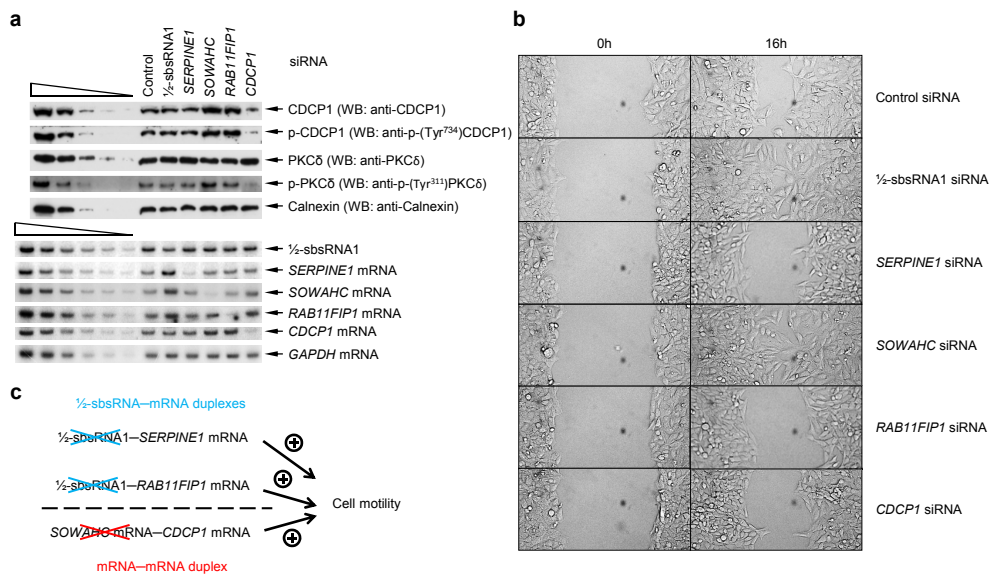
b (for Fig. 3c, d)



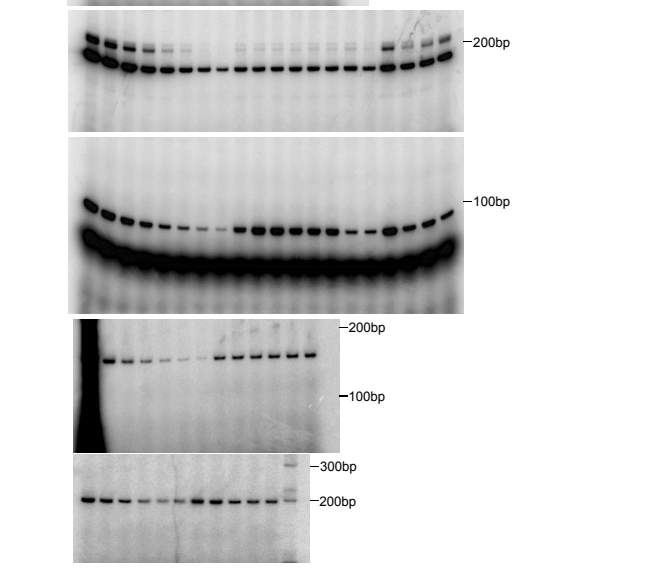
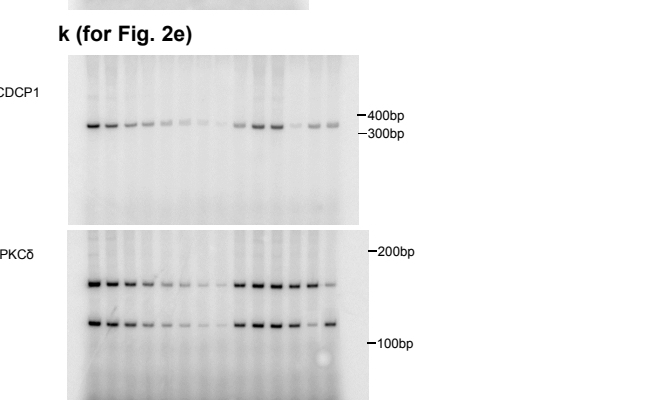
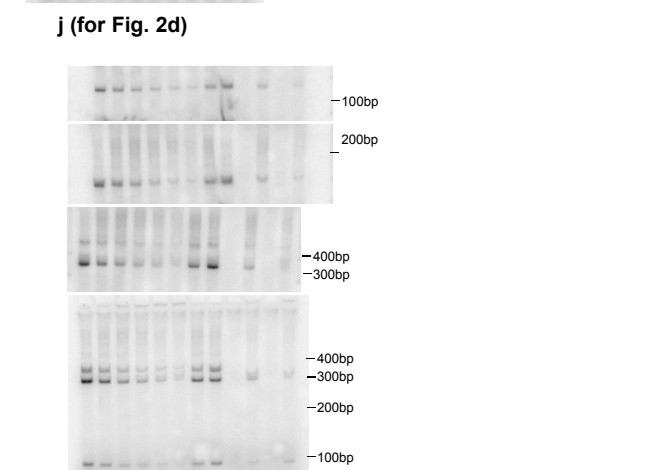
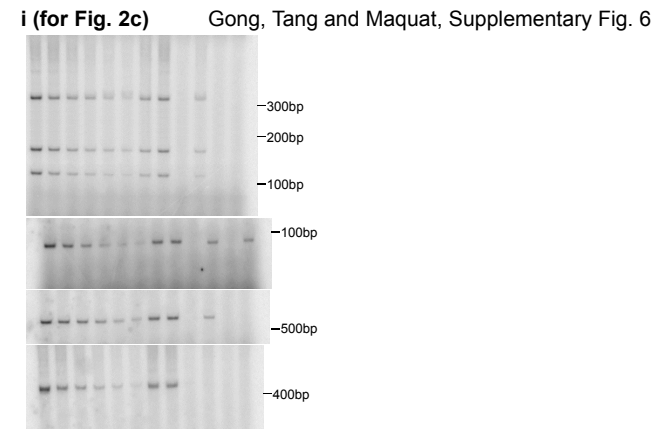
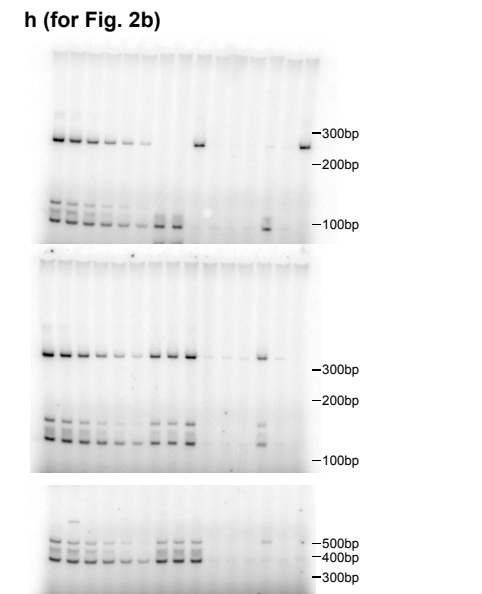
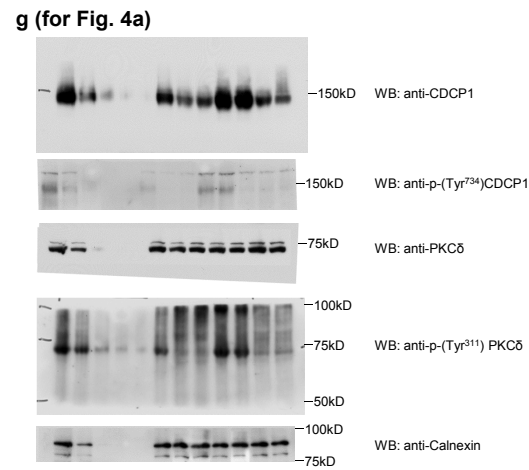
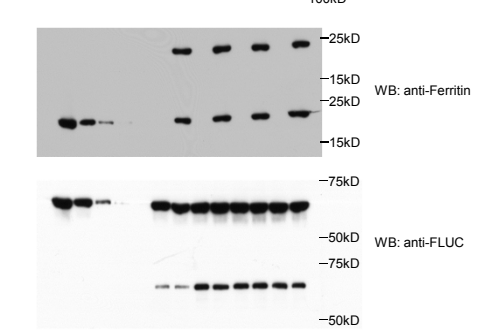
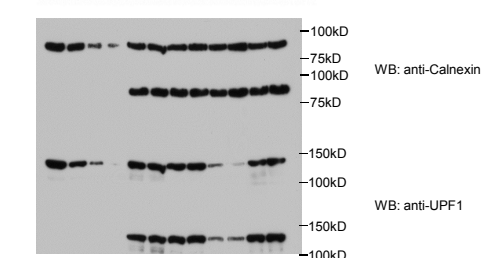
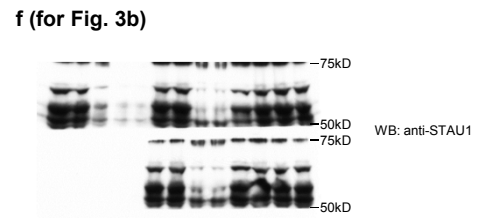
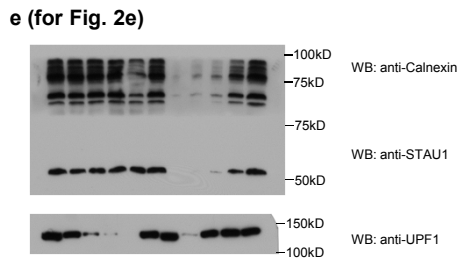
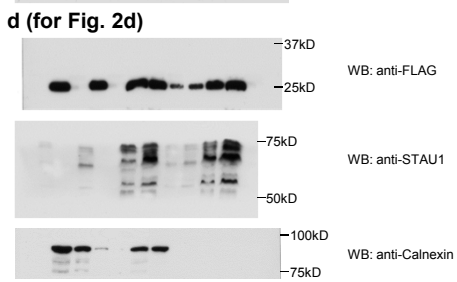
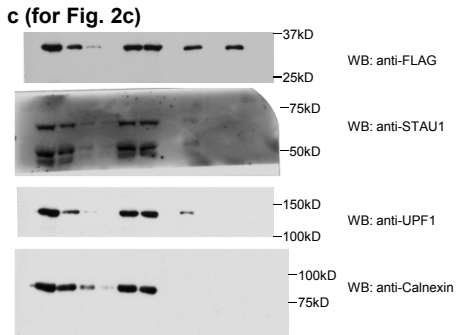
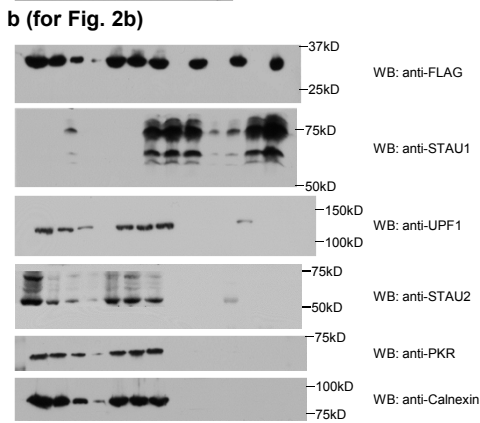
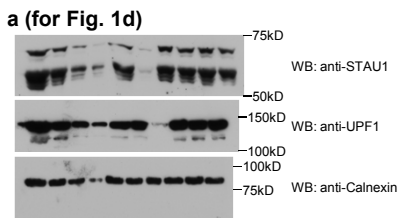
c (for Fig. 3c, d)

mRNA	Control		STAU1		UPF1		GI	
	Df	Hemin	Df	Hemin	Df	Hemin	Df	Hemin
FLUC-AS 3' UTR	100	104±9	299±19	276±13	301±14	285±12	243±17	248±11
IRE-GI	100	48±5	101±5	93±9	99±4	83±7	19±2	14±3

Supplementary Figure 4 | Evidence that hemin and deferoxamine mesylate, respectively, promote and inhibit IRE-GI mRNA translation. **a**, RT-sqPCR of RNA from HeLa cells that were cultured in DMEM supplemented with 10% FBS and 100 μ M of deferoxamine mesylate (Df) and subsequently in DMEM supplemented with 10% FBS and 100 μ M of either Df or hemin for 18 h. HeLa cells stably express either IRE-GI Norm mRNA, which does not contain a premature termination codon (PTC) and is not targeted for nonsense-mediated mRNA decay (NMD), or IRE-GI Ter mRNA, which does contain a PTC and is targeted for NMD. The level of IRE-GI Norm or Ter mRNA was normalized to the level of cellular *SMG7* mRNA, and the normalized level of IRE-GI Norm or IRE-GI Ter mRNA in the presence of Df was defined as 100. Data reveal that the normalized level of IRE-GI Ter mRNA is ~94% the level of IRE-GI Norm mRNA in the presence of Df but only ~12% of the level of IRE-GI Norm mRNA in the presence of hemin, consistent with Df inhibiting IRE-GI mRNA translation. **b**, Phosphorimages and quantitations of RT-sqPCR data shown as histograms in Fig. 3c and d. **c**, RT-qPCR data using RT samples analyzed in **b**. # of independently performed experiments = 3, $P < 0.05$ (one-tail *t*-test).



Supplementary Figure 5 | Evidence that mRNA–mRNA duplexes and ½-sbsRNA–mRNA duplexes that are targeted for SMD contribute to keratinocyte wound healing. a, Western blotting (WB) and RT-sqPCR analyses of lysates of human HaCaT keratinocytes that had been transiently transfected with the specified siRNA essentially as in Fig. 2c. Calnexin and *GAPDH* mRNA represent loading controls. **b,** Phase-contrast microscopy, which measured the rate of HaCaT keratinocyte wound healing. After transfection with the specified siRNA, cells were scrape-injured at 0 h and analyzed at 0 h and 16 h. **c,** Model for how mRNA–mRNA duplexes and ½-sbsRNA–mRNA duplexes contribute to wound healing. Arrows with plus signs specify activation, and red or blue Xs denote downregulation of ½-sbsRNA1 or *SOWAHC* mRNA, respectively. # of independently performed experiments = 3, P <0.05 (one-tail *t*-test).



Supplementary Figure 6 | Original images of gels, autoradiographs and blots.

Supplementary Table 1 | Computationally derived ΔG of DuplexFold-predicted duplexes that form between the 3' UTR Alu elements of the specified ensemble transcript pairs.

Table format:

ENSG00000XXXXXX(Tab)ENSG00000XXXXXX(Tab) ΔG value

ENSG00000YYYYYY(Tab)ENSG00000YYYYYY(Tab) ΔG value

Supplementary Table 2 | ΔG of predicted duplexes formed between the 3'UTR Alu element of each specified ensemble transcript and the 3'UTR Alu element of each of three proven SMD targets.

Supplementary Table 3 | Primers used in RT-sqPCR or RT-qPCR.

Supplementary Table 4 | Length of 3'UTR and siRNA annealing site(s) for each analyzed mRNA.